IOP Publishing Physics in Medicine and Biology

Phys. Med. Biol. **57** (2012) 5441–5458 doi:10.1088/0031-9155/57/17/5441

On the beam direction search space in computerized non-coplanar beam angle optimization for IMRT—prostate SBRT

Linda Rossi[1,2], **Sebastiaan Breedveld**[1], **Ben J M Heijmen**[1], **Peter W J Voet**[1], **Nico Lanconelli**[2] **and Shafak Aluwini**[1]

[1] Department of Radiation Oncology, Erasmus MC Rotterdam, Groene Hilledijk 301, 3075 EA Rotterdam, the Netherlands
[2] Alma Mater Studiorum, Department of Physics, Bologna University, Italy

E-mail: l.rossi@erasmusmc.nl and s.breedveld@erasmusmc.nl

Received 12 April 2012, in final form 29 June 2012
Published 3 August 2012
Online at stacks.iop.org/PMB/57/5441

Abstract

In a recent paper, we have published a new algorithm, designated 'iCycle', for fully automated multi-criterial optimization of beam angles and intensity profiles. In this study, we have used this algorithm to investigate the relationship between plan quality and the extent of the beam direction search space, i.e. the set of candidate beam directions that may be selected for generating an optimal plan. For a group of ten prostate cancer patients, optimal IMRT plans were made for stereotactic body radiation therapy (SBRT), mimicking high dose rate brachytherapy dosimetry. Plans were generated for five different beam direction input sets: a coplanar (CP) set and four non-coplanar (NCP) sets. For CP treatments, the search space consisted of 72 orientations (5° separations). The NCP CyberKnife (CK) space contained all directions available in the robotic CK treatment unit. The fully non-coplanar (F-NCP) set facilitated the highest possible degree of freedom in selecting optimal directions. CK^{+} and CK^{++} were subsets of F-NCP to investigate some aspects of the CK space. For each input set, plans were generated with up to 30 selected beam directions. Generated plans were clinically acceptable, according to an assessment of our clinicians. Convergence in plan quality occurred only after around 20 included beams. For individual patients, variations in PTV dose delivery between the five generated plans were minimal, as aimed for (average spread in V_{95}: 0.4%). This allowed plan comparisons based on organ at risk (OAR) doses, with the rectum considered most important. Plans generated with the NCP search spaces had improved OAR sparing compared to the CP search space, especially for the rectum. OAR sparing was best with the F-NCP, with reductions in rectum D_{Mean}, $V_{40\text{Gy}}$, $V_{60\text{Gy}}$ and $D_{2\%}$ compared to CP of 25%, 35%, 37% and 8%, respectively. Reduced rectum sparing with the CK search space compared to F-NCP could be largely compensated by expanding CK with beams with relatively large direction components along the superior–inferior axis (CK^{++}). Addition

of posterior beams ($CK^{++} \rightarrow$ F-NCP) did not lead to further improvements in OAR sparing. Plans with 25 beams clearly performed better than 11-beam plans. For CP plans, an increase from 11 to 25 involved beams resulted in reductions in rectum D_{Mean}, V_{40Gy}, V_{60Gy} and $D_{2\%}$ of 39%, 57%, 64% and 13%, respectively.

(Some figures may appear in colour only in the online journal)

1. Introduction

Stereotactic body radiation therapy (SBRT) involves hypofractionated delivery of high radiation doses and requires highly conformal treatment plans and optimal geometrical precision in daily dose delivery (Blomgren *et al* 1995). Hypofractionation may result in a treatment benefit for prostate cancer, as the α/β ratio could be as low as 1.5 (Miralbell *et al* 2012, Brenner and Hall 1999, Fowler *et al* 2001, King and Fowler 2001). Several randomized studies have demonstrated advantages of moderate hypofractionation in prostate cancer (Yeoh *et al* 2011, Arcangeli *et al* 2011, Pollack *et al* 2006, Norkus *et al* 2009).

Based on promising results with the strongly hypofractionated prostate high dose rate (HDR) brachytherapy (Grills *et al* 2004, Demanes *et al* 2005), interest has grown in developing non-invasive external beam radiotherapy (EBRT) techniques with as little as four fractions. Several of these studies were based on the robotic CyberKnife (CK) treatment unit (Accuray, Inc.) with its image-guided tumor tracking technology and easy use of non-coplanar (NCP) beams (King *et al* 2003, 2011, Katz and Santoro 2009, Freeman *et al* 2010, Townsend *et al* 2011, Kilby *et al* 2010, Fuller *et al* 2008, Freeman and King 2011, Jabbari *et al* 2012, Aluwini *et al* 2010, Fuller *et al* 2011).

The impact of beam angle optimization on the quality of treatment plans has been investigated in many studies (Pugachev and Xing 2001, Aleman *et al* 2009, Woudstra and Storchi 2000, de Pooter *et al* 2008, Voet *et al* 2012a, van de Water *et al* 2011). To our knowledge, very little is known about the importance of the extent of the beam angle search space in computer optimization of beam orientations, especially for NCP techniques.

Computer optimization of beam angles has been investigated for many years in our institution (Woudstra and Storchi 2000, de Pooter *et al* 2008, Voet *et al* 2012a, van de Water *et al* 2011). Most papers relate to 3D conformal techniques (Woudstra and Storchi 2000, de Pooter *et al* 2008, Voet *et al* 2012a), or to CK treatments with circular cones (van de Water *et al* 2011). Recently, we developed a new algorithm, designated 'iCycle', (Breedveld *et al* 2012), for multi-criterial optimization of beam angles and IMRT fluence profiles. In this study, we have used iCycle to investigate the importance of the beam angle search space in computer optimization of prostate SBRT plans that mimic HDR brachytherapy dose distributions. Plan comparisons were made for five different search spaces, including one with only CP directions and one with the orientations available at the CK.

2. Material and methods

2.1. Patients

Planning CT scans of ten prostate cancer patients, previously treated in our institution with the CK, were included in this study. Patients were treated with a dose of 38 Gy, delivered

in four fractions with a dose distribution that resembled prostate HDR brachytherapy. The CT-scan slice distances were 1.5 mm, the average scan length was 47.4 ± 6.7 cm (range: 35.7–55.7 cm). PTVs included the entire delineated GTV plus a 3 mm margin. The average volume was 90.8 ± 23.1 cc (range: 69.5–145.4 cc). Within the GTV, the peripheral zone (PZ) was defined with the help of MR images. Patients had four implanted markers for image guidance and were treated supine with their feet toward the robotic manipulator.

2.2. iCycle

All treatment plans were generated with iCycle, our novel in-house developed algorithm for automated, multi-criterial optimization of beam angles and IMRT fluence profiles. The algorithm is described in detail in Breedveld *et al* (2012). Here a brief summary of its features is provided.

Fully automated plan generation with iCycle is based on a 'wish-list', defining hard constraints that are strictly met and prioritized objectives (Breedveld *et al* 2007). The higher the priority of an objective, the higher the chance that the goal will be approached closely, reached or even exceeded. Furthermore, a list of candidate beam orientations for inclusion in the plan is needed. The beam direction search spaces and wish-list used in this study are described in detail below in the sections 2.3 and 2.4, respectively. A plan generation starts with zero beams. Optimal directions are sequentially added to the plan in an iterative procedure, up to a user-defined maximum number of beams. After each beam addition, iCycle generates a Pareto optimal IMRT plan including the beam directions selected so far. Consequently, plan generation for a patient always results in a series of Pareto optimal plans with increasing numbers of beams. For example, in this study the selected maximum number of beams is 30, resulting for each case in Pareto optimal IMRT plans with 30, 29, 28, 27, . . . beams. By design, addition of a beam improves plan quality regarding the highest prioritized objective that can still be improved on (Breedveld *et al* 2012).

2.3. Investigated beam direction input sets (search spaces)

In this study, the isocenter was placed in the center of the tumor. Beam directions were defined by straight lines (beam axes) connecting the isocenter with focal spot positions situated on a sphere centered around the isocenter. The five investigated beam direction search spaces were defined as follows.

(i) CP (coplanar): 72 equi-angular orientations in the axial plane through the isocenter, covering 360° around the patients (angular separation 5°).

(ii) CK (used by the CK robotic treatment unit): graphical presentation shown in figure 1. The set consists of 117 directions. Interesting features are the absence of beams with a large posterior component (upper-right panel in figure 1: available directions in the axial plane are limited to [−110°,110°]), and the asymmetry in the beam direction set (lower-left panel in figure 1) related to the asymmetric position of the robotic manipulator relative to the treatment couch.

(iii) F-NCP (fully non-coplanar): largest set of all five, theoretical, i.e. not related to a particular treatment device. Ideally, it should represent the search space as defined by all focal spots on a complete sphere around the isocenter. In the axial plane, through the isocenter, the angular distance between directions is 5° (F-NCP includes CP). NCP directions are separated by 10°. However, iCycle removes the NCP treatment beams that enter (partially) through the end of the CT dataset, which limits the available number of beam directions due to the finite lengths of the CT data sets (section 2.1). Because of this limitation, the

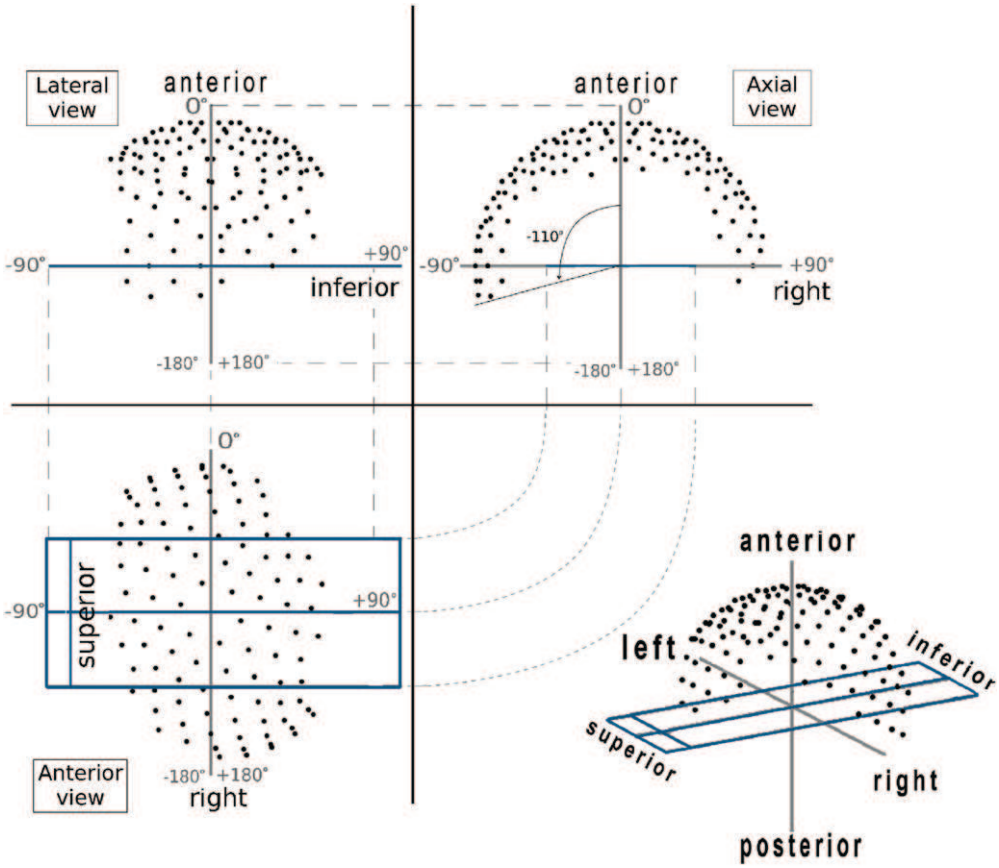

Figure 1. CK search space. The dots represent focal spot positions.

maximum deviation from the AP-axis in the sagittal plane is around 55°. F-NCP includes around 500 beam orientations, depending on the patient.

(iv) CK^{++}: as F-NCP, however excluding (*only*) directions with a posterior component outside the borders of the CK search space. In the axial plane, this results in exclusion of beams outside the [−110°,110°] range (figure 1, upper-right panel). Depending on the patient, CK^{++} has around 300 beam directions.

(v) CK^{+}: as F-NCP, however excluding *all* directions outside the borders of the CK search space (figure 1). Because of the higher focal spot density, the number of available directions in CK^{+} is higher than that for CK, i.e. 186 versus 117.

2.4. iCycle generation of prostate SBRT plans

iCycle was used to optimize beam angles and intensity profiles for high-quality SBRT plans, mimicking HDR brachytherapy dose distributions. Table 1 shows the applied wish-list with planning constraints and objectives in the upper and lower parts, respectively. The wish-list was established in a trial-and-error procedure to ensure for this patient population generation of high-quality plans with the desired balance between the clinical objectives (see also Voet

Table 1. Applied wish-list for all study patients. For definition of rings 1, 2 and 3, see section 2.4.

Constraints	Structure	Type	Limit	
	PTV	Maximum	59–69 Gy	
	Rectum	Maximum	38 Gy	
	Urethra	Maximum	40 Gy	
	Bladder	Maximum	41.8 Gy	
	Penis scrotum	Maximum	4 Gy	
	Penis scrotum	Mean	2 Gy	
	Ring 2	Maximum	15 Gy	
	Ring 1	Maximum	20 Gy	
Objectives Priority	Structure	Type	Goal	Parameters
1	PTV	LTCP	1	$D_p = 34$–38 Gy, $\alpha = 0.7$, sufficient = 0.003–0.20
2	PTV	LTCP	4	$D_p = 55$–60.8 Gy, $\alpha = 0.1$–0.2, sufficient = 4–26
3	Rectum	Mean	0 Gy	
4	PZ	LTCP	1	$D_p = 45$ Gy, $\alpha = 0.9$
5	Urethra	Mean	0 Gy	
6	Bladder	Mean	0 Gy	
7	Ring 3	Maximum	15 Gy	
8	Rectum	Maximum	30 Gy	
9	Bladder	Maximum	35 Gy	
10	Penis scrotum	Maximum	0	
11	Left and right femur head	Maximum	24	

et al (2012a) and Breedveld *et al* (2012)). Most important clinical goals were adequate PTV coverage and a maximally reduced rectum dose.

The two highest priority objectives, defined with logarithmic tumor control probability (LTCP) functions (Alber and Reemtsen 2007), aimed at adequate PTV dose delivery. The first focused on control of PTV doses around 34–38 Gy, while the second mainly steered PTV doses around 55–60.8 Gy. For each patient, the goal was to generate, for all five beam angle search spaces (section 2.3), plans with highly similar PTV dose delivery, all close to the dose delivered in the clinical plan, allowing the comparison of search spaces based on OAR plan parameters. To this purpose, prior to the final plan generations for a patient, trial plans were generated to fine-tune the LTCP sufficient and α parameters (Breedveld *et al* 2009) for a PTV maximum dose constraint (table 1) equal to the maximum dose in the clinical plan. For each patient, a fixed set of sufficient, α, and PTV maximum dose values was used for the final plan generation for all five search spaces.

As in clinical practice, reduction of rectum dose delivery was the most important OAR objective (priority 3 in table 1), aiming at a mean dose of 0 Gy. With this choice, the optimizer would only reduce doses to other OARs to the extent that this would not compromise reaching the lowest possible mean rectum dose. Other OAR considered with lower priorities were urethra, bladder, penis, scrotum and femoral heads. Other structures, *rings*, were defined to control and reduce the dose to healthy tissues: 'ring 1' includes all tissues between 2 and 3 cm from the PTV; 'ring 2' includes all tissues between the body contour and the body contour-2 cm and 'ring 3' is referred to all tissues in between ring 1 and ring 2. Hard constraints on ring 1 and ring 2 had to enforce a steep dose fall-off outside the target and to limit the entrance dose, respectively. The priority 7 objective on ring 3 aimed at dose reduction to healthy tissues, also if not part of an OAR.

For all beam direction search spaces considered in this study, the simulations assumed that beam collimation was performed with a dynamic multi-leaf collimator (MLC) with a 5 mm leaf width. The maximum field size was 10×12 cm^2 and leaves had full interdigitation and overtravel. For dose calculations, percentual depth dose curves and profiles of an Elekta Synergy 6 MV beam, collimated with an MLCi2, were used. Pencil beam kernels for optimization were derived as described in Storchi and Woudstra (1996). Equivalent path length correction was used for inhomogeneity correction.

2.5. Details on plan evaluation and comparison

The plans in this study were evaluated by a clinician (SA) to check clinical acceptability. In accordance with the ICRU-83 report (ICRU 2010), $D_{2\%}$ and $D_{98\%}$ were reported instead of maximum and minimum doses, respectively. In line with QUANTEC findings (Michalski *et al* 2010), rectum dose delivery reporting included $V_{40\mathrm{Gy}}$ and $V_{60\mathrm{Gy}}$, calculated by first converting delivered doses to a 2 Gy/fraction regime using an alpha/beta parameter of 3 Gy. Apart from doses delivered to the PTV, PZ and OARs, we also analyzed $V_{10\mathrm{Gy}}$, $V_{20\mathrm{Gy}}$ and $V_{30\mathrm{Gy}}$, the patient volumes receiving more than 10, 20 and 30 Gy, respectively. Evaluations also included the conformity index (CI) calculated as the ratio of the total tissue volume receiving 38 Gy or more and the PTV (almost 100% of the PTV received 38 Gy, see section 3). Hard constraints on dose delivery to the penis and the scrotum guaranteed negligible doses to these structures in all plans (table 1), which are not reported in section 3.

As described in section 2.4, for each patient we aimed at highly similar PTV doses for all five search spaces. In section 3, it is demonstrated that differences were indeed very small. For this reason, comparison of plans and search spaces could be based on doses delivered to healthy tissues with the rectum being the most important one. The two-sided Wilcoxon signed-rank test was used to compare plan parameters in the various search spaces. A p-value of <0.05 was defined as statistically significant.

2.6. Treatment time calculation for the CK search space

We calculated treatment times for the hypothetical situation that the CK would be equipped with an MLC. Treatment times consist of beam-on time, linac travel time and imaging time. For calculation of beam-on times, we used a leaf sequencing algorithm described in van Santvoort and Heijmen (1996), assuming a linac output of 1000 MU min^{-1} (as available for the current CK), a maximum leaf speed of 2.5 cm s^{-1} and full leaf interdigitation and overtravel (see also section 2.4). Leaf synchronization was not applied. The linac travel time is the time to travel through all selected focal spot positions. However, CK movements are not totally free, i.e. it cannot freely travel from each spot position to any other, but it sometimes has to pass unselected (but allowed, figure 1) positions to reach a next selected position. The applied travel time calculation algorithm selects the shortest path, considering all possible movements between spot positions (van de Water *et al* 2011). For the treatment time calculations, we assumed that prior to dose delivery from a focal spot position, images were acquired to verify and, if needed, correct alignment of the beam to be delivered with the current tumor position. Imaging time takes only 2 s. However, CK has some node positions from which it is not possible to take an image. To handle this, the machine has to travel to the nearest node position from which imaging is allowed and come back to the delivery position. This aspect was also considered in the calculation of the treatment times.

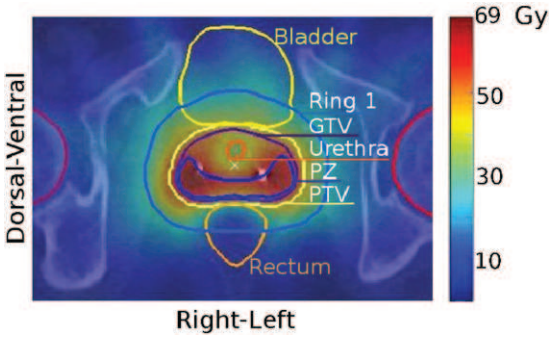

Figure 2. Axial dose distribution for the 25-beam plan generated with the CK search space for the first study patient. For definition of ring 1, see section 2.4.

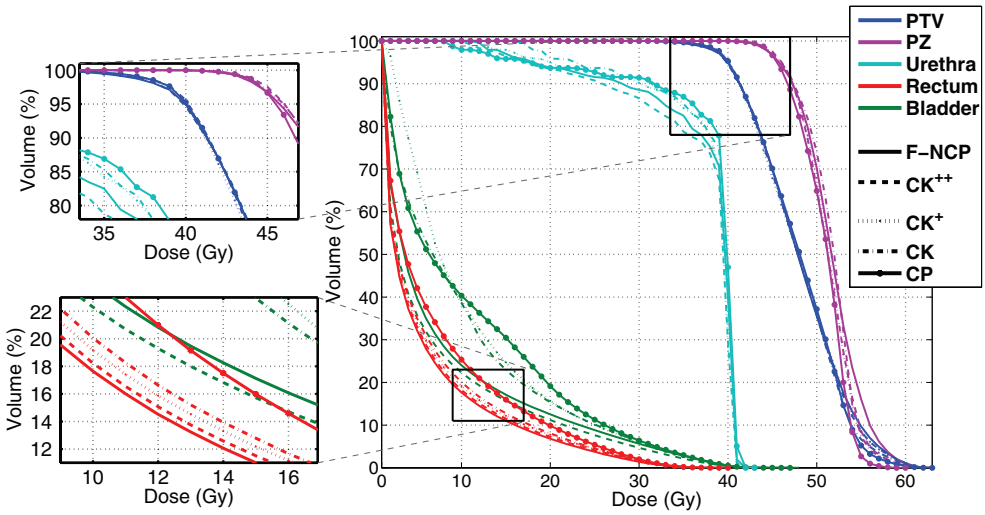

Figure 3. Dose volume histogram (DVH) comparison for patient 1 for five 25-beam plans, each generated for one of the five studied search spaces.

3. Results

3.1. Generated plans

In this section, plans and analyses performed for the first study patient are described in some detail to provide examples of the investigations performed for all ten patients.

Figure 2 shows an axial dose distribution for the 25-beam plan generated with the CK search space. Clearly visible are the high degree of rectum sparing, the reduced dose in the urethra and the increased dose in the PZ, as enforced by the applied wish-list (table 1).

Figure 3 shows DVHs for the 25-beam plans generated with each of the five search spaces in this study. As aimed for (section 2.4), PTV coverages for the five plans were highly similar (upper-left zoom). Rectum sparing was best for F-NCP and CK^{++}, while for the CP plan, rectum dose was clearly the highest (lower-left zoom). F-NCP was best for bladder and CK^{++}

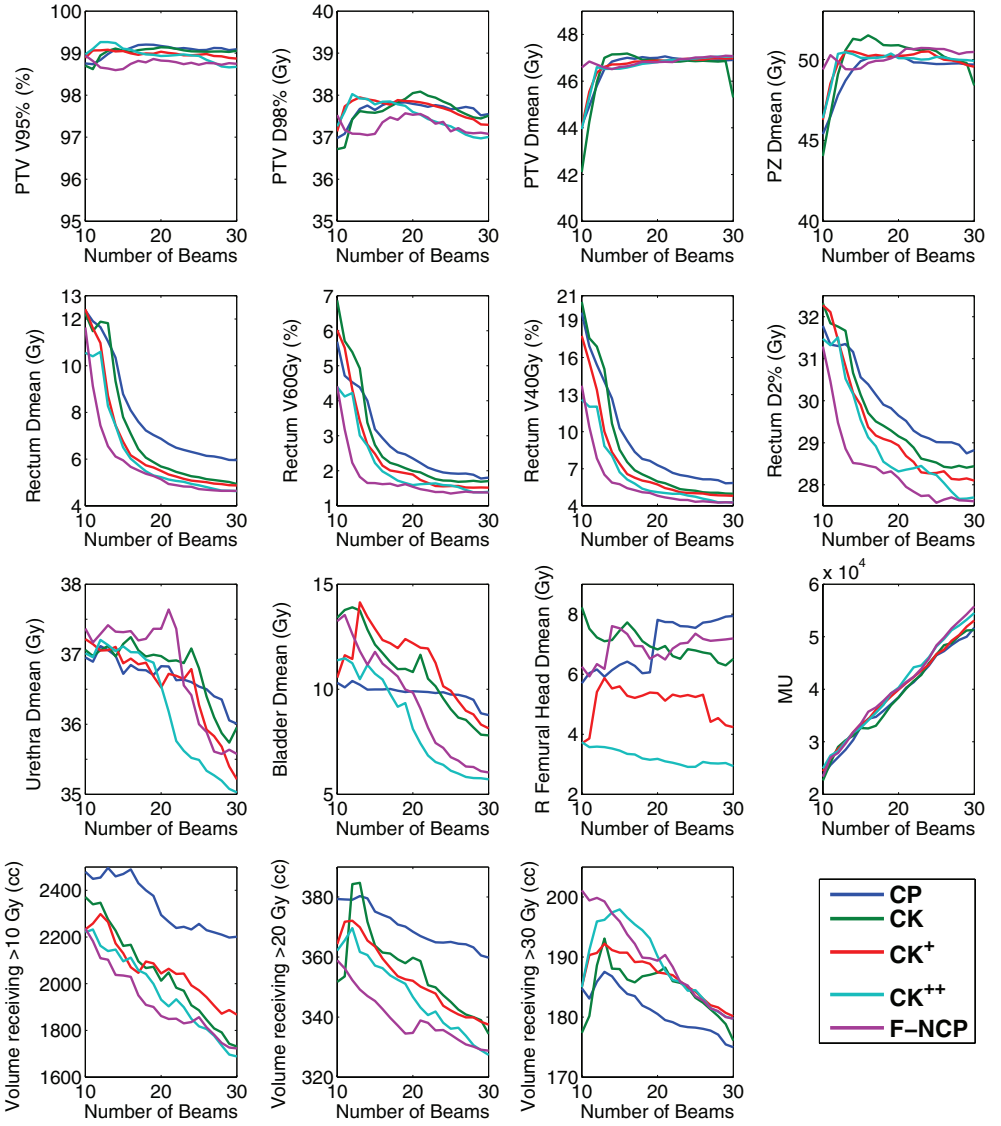

Figure 4. Dosimetrical results for patient 1 for plans with 10 up to 30 beams for the five studied input beam sets.

for urethra, with F-NCP second. Obviously, plans for the NCP search spaces with the largest extents (F-NCP and CK^{++}) were most favorable for this patient.

Figure 4 shows plan parameters as a function of the number of beams in the plan. For all beam numbers, PTV coverage was very similar for the five search spaces. The second row shows that for all search spaces, rectum dose parameters improved with increasing numbers of beams, with some leveling off between 15 and 20 beams. Also, bladder D_{Mean}, urethra D_{Mean}, $V_{10\mathrm{Gy}}$, $V_{20\mathrm{Gy}}$ and $V_{30\mathrm{Gy}}$ improved with increasing numbers of beams. A very similar behavior of plan quality on numbers of involved beams was seen for all ten patients in this study. In the following section, population data will be provided for PTV and rectum.

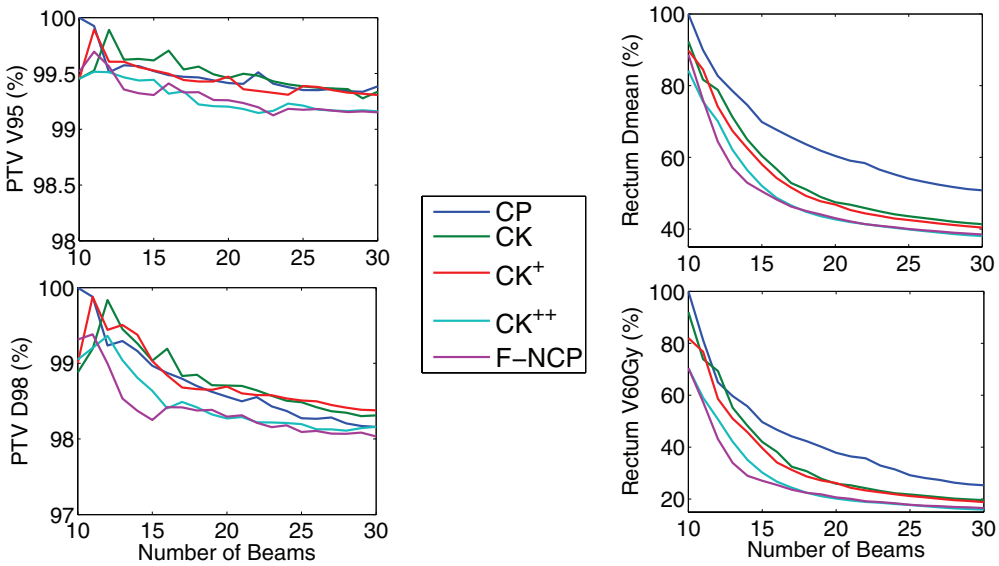

Figure 5. Population-averaged PTV (left) and rectum (right) plan parameters as a function of beam number, for 10–30-beam plans. All percentages are relative to absolute population mean values of the CP ten-beam plan, i.e. PTV $V_{95} = 99.5\%$, PTV $D_{98} = 37.8$ Gy, rectum $D_{\text{Mean}} = 11.3$ Gy and rectum $V_{60\text{Gy}} = 8\%$.

3.2. Plan quality versus number of beams in plans, PTV and rectum

The left panel in figure 5 shows the average PTV V_{95} and PTV D_{98} for the ten study patients, as a function of the number of beams in the plans, normalized to the CP ten-beam plan. For each search space, these quantities are largely independent of the number of beams (normalized values differ up to 0.8% and 2% for average PTV V_{95} and D_{98}, respectively). The trend to slightly reduced PTV dose delivery with increasing number of beams is (partly) related to enhanced urethra sparing with more beams (no data presented). For all beam numbers, these PTV dose parameters are also highly similar for the five search spaces with variations up to less than 0.5%. The right panel demonstrates substantial differences between the search spaces in population-averaged rectum D_{Mean} and rectum $V_{60\text{Gy}}$, with the lowest values for F-NCP and the least favorable values for CP. For 20 beams, F-NCP-averaged rectum D_{Mean} and $V_{60\text{Gy}}$ were 29% and 45% lower compared to CP. For all five search spaces, rectum dose improved with an increasing number of beams. None of the curves in the right panel fully levels off, but reductions with beam number are clearly most prominent up to around 20 beams. In the remainder of this paper, data for 25-beam plans will be reported, unless stated otherwise.

3.3. 25-beam plans—CP versus NCP beam direction search spaces

Table 2 provides a comparison of the CP search space with the four NCP spaces regarding plan parameters of the generated 25-beam plans.

As aimed for (section 2.4), differences in PTV D_{Mean}, PTV V_{95} and PTV $D_{98\%}$ between the five search spaces were clinically and/or statistically insignificant. Compared to CP, only PTV $D_{2\%}$ was around 3% higher for NCP set-ups ($p < 0.05$), but clinically, these increases were considered unimportant. No relevant differences were observed in the PZ parameters.

Table 2. Comparison of dosimetric plan parameters of the generated 25-beam plans, for the five investigated beam angle search spaces. Mean values, standard deviations (SD) and ranges refer to the ten patients in the study. The first data column reports the results obtained with the CP search space. In the next columns, percentage differences of the other spaces with CP are shown, i.e. 100∗(other_search_space—CP)/CP. (*) refers to all tissues receiving >10, >20 or >30 Gy. Statistically non-significant (NS) for $p > 0.05$. The bold values are mean values averaged on 10 patients results.

	CP		F-NCP − CP (%)			CK^{++} − CP (%)			CK^{+} − CP (%)			CK − CP (%)		
	Mean ± 1SD	[Range]	ΔMean ± 1SD	[Range]	p	ΔMean ± 1SD	[Range]	p	ΔMean ± 1SD	[Range]	p	ΔMean ± 1SD	[Range]	p
Target														
PTV D_{Mean}	**46.7** ± 2.2 (Gy)	[44.1, 50.9]	**0.4** ± 1.2	[−0.4, 3.4]	NS	**0.6** ± 1.3	[−0.7, 4.1]	NS	**0.3** ± 1.0	[−0.3, 3.0]	0.01	**0.3** ± 0.8	[−0.4, 2.4]	NS
PTV V_{95}	**99.0** ± 0.6 (%)	[97.4, 99.7]	**−0.3** ± 0.5	[−1.5, 0.1]	NS	**−0.3** ± 0.4	[−1.5, 0.1]	.006	**−0.1** ± 0.3	[−0.8, 0.2]	NS	**−0.1** ± 0.3	[−0.8, 0.2]	NS
PTV $D_{98\%}$	**37.2** ± 0.7 (Gy)	[35.7, 38.1]	**−0.3** ± 1.2	[−2.4, 1.3]	NS	**−0.2** ± 1.2	[−2.5, 1.3]	NS	**0.1** ± 1.1	[−1.8, 1.2]	NS	**0.1** ± 0.9	[−1.7, 1.0]	NS
PTV $D_{2\%}$	**56.5** ± 3.8 (Gy)	[51.0, 63.5]	**2.7** ± 4.0	[−1.1, 12.2]	.02	**3.2** ± 4.8	[−3.5, 14.3]	NS	**3.1** ± 4.1	[−0.0, 13.5]	0.01	**3.3** ± 4.0	[0.1, 13.1]	0.01
PZ D_{Mean}	**50.4** ± 2.3 (Gy)	[47.0, 54.6]	**0.9** ± 2.0	[−1.5, 4.3]	NS	**1.3** ± 2.1	[−2.2, 5.6]	NS	**0.5** ± 1.9	[−2.0, 3.1]	NS	**0.3** ± 1.7	[−1.7, 2.3]	NS
PZ $D_{98\%}$	**37.2** ± 0.7 (Gy)	[35.7, 38.1]	**−0.3** ± 1.2	[−2.4, 1.3]	NS	**−0.2** ± 1.2	[−2.5, 1.3]	NS	**0.1** ± 1.1	[−1.8, 1.2]	NS	**0.1** ± 0.9	[−1.7, 1.0]	NS
Rectum														
D_{Mean}	**6.2** ± 2.1 (Gy)	[3.4, 10.2]	**−25.0** ± 9.0	[−44.6, −13.8]	0.002	**−25.2** ± 8.5	[−42.8, −13.5]	0.002	**−20.2** ± 8.1	[−39.3, −9.5]	0.002	**−18.5** ± 8.0	[−36.9, −8.4]	0.002
V_{40Gy}	**6.6** ± 2.7 (%)	[3.1, 12.1]	**−34.9** ± 14.2	[−68.9, −18.8]	0.002	**−35.2** ± 13.5	[−67.4, −19.7]	0.002	**−25.8** ± 13.3	[−58.7, −11.5]	0.002	**−23.2** ± 14.1	[−57.8, −10.1]	0.002
V_{60Gy}	**2.4** ± 1.1 (%)	[0.7, 4.3]	**−36.5** ± 19.3	[−78.4, −16.5]	0.002	**−35.4** ± 20.1	[−78.3, −11.3]	0.002	**−22.6** ± 21.8	[−66.4, 3.7]	0.004	**−21.4** ± 20.8	[−68.0, −1.7]	0.002
$D_{2\%}$	**29.5** ± 2.2 (Gy)	[25.4, 32.1]	**−7.5** ± 4.3	[−17.4, −2.6]	0.002	**−7.6** ± 4.0	[−16.8, −2.7]	0.002	**−4.4** ± 3.3	[−12.1, −1.7]	0.002	**−3.9** ± 3.6	[−12.6, −0.4]	0.002
Urethra														
D_{Mean}	**32.2** ± 3.5 (Gy)	[26.4, 36.5]	**−0.4** ± 1.3	[−2.2, 2.1]	NS	**−0.3** ± 2.0	[−2.9, 3.7]	NS	**−0.3** ± 1.6	[−2.5, 3.0]	NS	**−0.4** ± 1.2	[−2.5, 1.8]	NS
$D_{2\%}$	**40.0** ± 0.2 (Gy)	[39.8, 40.3]	**−0.4** ± 0.6	[−1.4, 0.5]	NS	**−0.4** ± 0.6	[−1.2, 0.3]	NS	**−0.4** ± 0.6	[−1.5, 0.3]	NS	**−0.3** ± 0.5	[−1.3, 0.5]	NS
Bladder														
D_{Mean}	**8.8** ± 2.4 (Gy)	[3.7, 12.6]	**−9.0** ± 18.4	[−43.6, 20.0]	NS	**−8.5** ± 23.3	[−46.5, 22.6]	NS	**11.2** ± 17.3	[−13.5, 44.3]	NS	**10.6** ± 18.7	[−17.1, 48.0]	NS
$D_{2\%}$	**34.4** ± 3.4 (Gy)	[25.4, 37.9]	**0.9** ± 1.6	[−2.6, 2.5]	NS	**0.1** ± 3.6	[−7.8, 4.2]	NS	**2.4** ± 2.1	[−1.0, 5.0]	0.01	**2.5** ± 1.7	[0.1, 5.2]	0.002
Femoral heads														
R D_{Mean}	**9.1** ± 2.7 (Gy)	[5.4, 14.5]	**−35.1** ± 21.5	[−67.8, −8.6]	0.002	**−34.2** ± 19.8	[−72.1, −14.1]	0.002	**−34.3** ± 15.5	[−62.9, −12.0]	0.002	**−20.8** ± 16.3	[−50.8, −2.4]	0.002
R $D_{2\%}$	**15.6** ± 0.7 (Gy)	[14.8, 17.1]	**−24.2** ± 13.9	[−46.2, −7.2]	0.002	**−23.9** ± 10.2	[−50.3, −14.8]	0.002	**−18.7** ± 4.5	[−29.2, −14.2]	0.002	**−9.7** ± 7.1	[−25.4, −1.5]	0.002
L D_{Mean}	**9.0** ± 2.5 (Gy)	[5.7, 13.2]	**−32.6** ± 26.9	[−76.1, 2.3]	0.004	**−42.4** ± 25.7	[−76.5, 3.5]	0.004	**−31.3** ± 19.6	[−62.9, 4.8]	0.004	**−23.3** ± 14.7	[−50.8, −7.1]	0.002
L $D_{2\%}$	**15.4** ± 0.8 (Gy)	[14.2, 16.8]	**−19.9** ± 15.0	[−56.6, −2.6]	0.002	**−22.2** ± 15.6	[−52.0, −6.5]	0.002	**−18.9** ± 13.8	[−47.4, 1.5]	0.004	**−9.8** ± 6.6	[−22.0, −0.6]	0.002
Other														
V_{10Gy}*	**2020** ± 331 (cc)	[1624, 2758]	**−17.0** ± 5.8	[−28.6, −9.4]	0.002	**−15.9** ± 7.2	[−28.0, −8.7]	0.002	**−13.4** ± 4.7	[−19.0, −3.7]	0.002	**−14.7** ± 3.6	[−21.1, −9.3]	0.002
V_{20Gy}*	**352** ± 63 (cc)	[285, 500]	**−8.3** ± 2.2	[−13.4, −6.1]	0.002	**−6.9** ± 2.0	[−10.0, −3.3]	0.002	**−5.3** ± 1.8	[−7.9, −2.2]	0.002	**−4.3** ± 1.7	[−7.0, −2.4]	0.002
V_{30Gy}*	**169** ± 31 (cc)	[137, 242]	**3.4** ± 2.5	[−2.1, 6.6]	0.006	**5.0** ± 2.7	[−0.1, 8.8]	0.004	**4.5** ± 2.3	[−0.2, 7.3]	0.004	**3.4** ± 2.0	[−0.4, 5.8]	0.004
CI	**1.2** ± 0.1	[1.1, 1.3]	**7.0** ± 2.9	[1.8, 11.4]	0.002	**9.2** ± 3.1	[4.4, 13.7]	0.002	**7.1** ± 2.2	[3.5, 10.6]	0.002	**5.5** ± 2.3	[2.7, 9.2]	0.002
MU	**43 533** ± 2694	[39264, 46572]	**8.4** ± 4.8	[4.1, 19.3]	0.002	**8.2** ± 6.6	[3.1, 23.1]	.002	**7.4** ± 6.0	[0.5, 19.5]	0.002	**6.9** ± 6.8	[−2.0, 22.0]	0.01

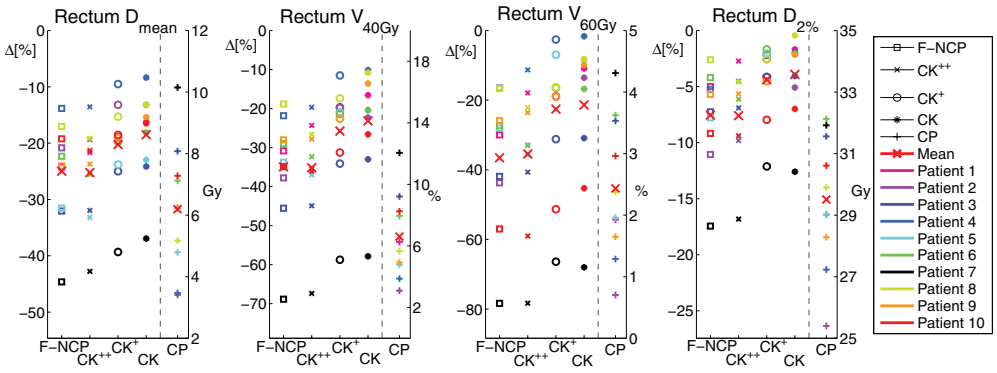

Figure 6. Comparison of the CP search space with the four NCP spaces for four rectum plan parameters. On the right of each panel, the CP absolute values for each patient are reported. The four columns on the left report the percentage differences for NCP search spaces with the CP plan. For all patients and all parameters, differences $\Delta[\%]$ are below zero, showing the improved rectum sparing with NCP beam search spaces. All plans are with 25 beams.

Because of this high similarity in target dose for the five search spaces, in the remainder of this paper, plan comparisons are focused on organs at risk and especially on the rectum.

The rectum population mean plan parameters were clearly the lowest for the four NCP search spaces (table 2). For the largest search space, F-NCP, population mean reductions relative to CP in rectum D_{Mean}, $V_{40\text{Gy}}$, $V_{60\text{Gy}}$ and $D_{2\%}$ were as large as 25.0%, 34.9%, 36.5% and 7.5%, respectively. For CK, these reductions were the smallest but still highly relevant (18.5%, 23.2%, 21.4% and 3.9%, respectively). Figure 6 demonstrates that the superiority of the NCP search spaces holds for all individual patients. Patient 7 had the highest CP rectum dose parameters, while percentual reductions with the NCP set-ups were also the highest (figure 6). Regression analyses showed, for all four NCP search spaces, increasing percentual reductions in rectum dose parameters for increasing CP parameters ($p = 0.001$–0.03), i.e. patients with less favorable CP rectum parameters had the largest reductions when switching to a NCP plan.

Population mean urethra doses were equal for all five search spaces (table 2). Differences between NCP spaces and CP in mean bladder dose were highly patient specific. F-NCP and CK^{++} had on average ≈9% lower mean bladder doses, while for CK^{+} and CK, mean bladder doses were around ≈11% higher compared to CP. None of these differences were statistically significant. With CP, doses in the femoral heads were already low, but substantial percentual reductions were seen for the NCP beam sets. Also, $V_{10\text{Gy}}$ and $V_{20\text{Gy}}$ were the lowest for the NCP sets.

$V_{30\text{Gy}}$, the total delivered number of MU and the CI were the only parameters for which CP plans did on average (slightly) better than NCP set-ups. $V_{30\text{Gy}}$ and MU were 3–5% and 8% lower in the CP plans. The mean CI in the CP plans for the ten study patients was 1.2, which increased to 1.27–1.31 for the NCP sets.

3.4. 25-beam plans—comparison of NCP search spaces

As described in detail in section 2.3, NCP search spaces increased in extent when going from CK to CK^{+} to CK^{++} and finally to F-NCP. Briefly, CK^{+} had the same boundaries as CK but a higher spot density, CK^{++} was an expansion of CK^{+} with beams with relatively large

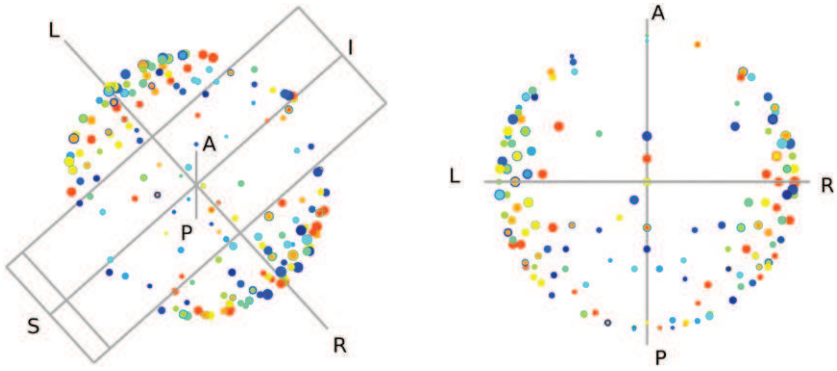

Figure 7. Selected focal spots/beams by iCycle for 25-beam F-NCP plans for all ten patients in a 3D (left) and an axial view (right). Colors refer to different patients and beam weights are proportional to the dot diameters.

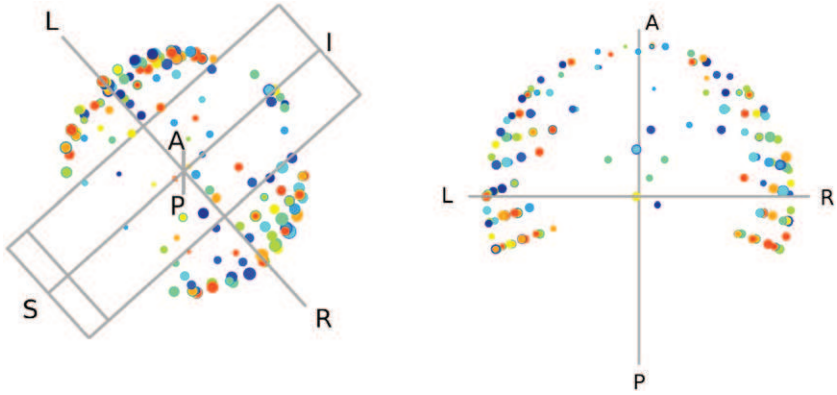

Figure 8. Selected focal spots/beams by iCycle for 25-beam CK^{++} plans for all ten patients in a 3D (left) and an axial view (right). Colors refer to different patients and beam weights are proportional to the dot diameters.

direction components along the superior–inferior axis and F-NCP was an extension of CK^{++}, making it the only NCP search space with posterior beams. In this section, changes in plan parameters related to these increases in degree of freedom for selecting optimal NCP beam angles are discussed.

CK $\rightarrow$ *CK*$^{+}$. As also visible in table 2, CK has the highest mean rectum dose parameters of the four NCP beam direction search spaces. Increasing the focal spot density did only marginally improve rectum dose delivery, although reductions in D_{Mean} of 2.2% and in $V_{40\text{Gy}}$ of 3.2% were statistically significant. For urethra and bladder, differences in delivered dose were negligible (table 2). Significant differences were found for femoral head doses. With CK^{+}, D_{Mean} and $D_{2\%}$ for right and left head decreased by 15%, 9%, 11% and 10%, respectively (p-values: 0.02, 0.04, 0.04, 0.03). Small, but statistically significant, differences were found for $V_{20\text{Gy}}$ (CK^{+} 1% lower, $p = 0.01$), $V_{30\text{Gy}}$ (CK^{+} 1.1% higher, $p = 0.02$) and for CI (CK^{+} 1.5% higher, $p = 0.01$).

$CK^{+} \rightarrow CK^{++}$. With this increase in search space, the population mean rectum D_{Mean}, $V_{40\text{Gy}}$, $V_{60\text{Gy}}$ and $D_{2\%}$ were reduced by as much as 6.8%, 12.0%, 16.9% and 3.5%, respectively ($p = 0.002$). Large improvement was also found for the bladder with a reduction in D_{Mean} of 26.9% ($p = 0.01$). $V_{20\text{Gy}}$ was also improved with CK^{++} (1.7%, $p = 0.002$). CI was slightly better for CK^{+} (2.3%, $p = 0.001$).

$CK^{++} \rightarrow$ F-NCP. Adding posterior beams by going from CK^{++} to F-NCP did not result in relevant further reductions in rectum dose (table 2). Very small improvements were seen for $V_{20\text{Gy}}$ (1.5%, $p = 0.006$), $V_{30\text{Gy}}$ (1.6%, $p = 0.001$) and CI (2.0%, $p = 0.004$).

3.5. 25-beam plans—distribution of selected beam orientations

Figure 7 shows selected beam directions for the 25-beam F-NCP plan of each individual study patient. Clearly, there is a preference for beams with a large lateral component. Comparison of the right panels of figures 7 and 8 shows that most high-weight beams in the F-NCP plans are within the CK^{++} search space. Apparently, beams with a large posterior component are not frequently selected or have low weights.

3.6. 25-beam plans—treatment times for the CK search space

Treatment times for the 25-beam CK plans were on average 18.1±0.5 min, including dose delivery, robot motion and imaging and set-up correction prior to delivery of each beam (section 2.6).

3.7. 11-versus 25-beam CP plans

As visible in figure 4 for patient 1 and in the right panel of figure 5 for the patient population, OAR plan parameters may substantially improve with increasing numbers of beams in the plans. On regular treatment units, IMRT plans are generally delivered with CP beam set-ups with $\leqslant$11 beams. Table 3 compares CP plans with 11 and 25 beams. Although differences in PTV parameters are statistically significant, they are small, and clinically the obtained PTV doses are considered highly comparable. An important consideration here is that the difference in PTV V_{95}, our most important parameter for PTV dose evaluation, is very small. The most striking differences were found for the rectum with improvements in D_{Mean}, $V_{40\text{Gy}}$, $V_{60\text{Gy}}$ and $D_{2\%}$ of 39.2%, 57%, 63.7% and 12.6% ($p = 0.002$), when increasing the number of beams from 11 to 25. Bladder D_{Mean} and $D_{2\%}$ reduced by 14.4% ($p = 0.002$) and 5.3% ($p = 0.004$), respectively, and $V_{10\text{Gy}}$ improved by 11.1% ($p = 0.002$). When switching to 25-beam plans, the MU increased on average by 75.7% ($p = 0.002$).

3.8. Calculation times

iCycle simulations were done in Matlab 7.12, R2011a, The Mathworks Inc., on a four-socket ten-core Intel Xeon E7. Plan optimization required ≈35 h to generate for one patient F-NCP plans with up to 25 beams, i.e. 25 complete plans have been generated and all data are individually available, and around ≈45 h for up to 30 beams. These times reduced to ≈15 and ≈25 h to generate CP treatment plans.

Table 3. Results for ten patients for 11- and 25-beam coplanar plans. The first column reports the results obtained with the 11-beam coplanar configuration. In the next columns, the percentage decreases from the 11-beam CP results are shown. (*) refers to all tissues receiving >10, >20 or >30 Gy.

	11 beams, CP		25 versus 11 beams, CP (%)		
	Mean ± 1SD	[Range]	ΔMean ± 1SD	[Range]	*p*-value
Target					
PTV D_{Mean}	**45.1** ± 1.0 (Gy)	[43.4, 46.7]	**3.4** ± 3.1	[0.2, 9.1]	0.002
PTV V_{95}	**99.4** ± 0.4 (%)	[98.7, 99.9]	**−0.5** ± 0.5	[−1.8, 0.3]	0.01
PTV $D_{98\%}$	**37.8** ± 0.5 (Gy)	[37.1, 38.6]	**−1.5** ± 1.4	[−3.9, 1.6]	0.02
PTV $D_{2\%}$	**52.8** ± 1.8(Gy)	[49.5, 56.1]	**7.0** ± 4.2	[1.6, 13.2]	0.002
PZ D_{Mean}	**48.1** ± 0.9 (Gy)	[46.5, 48.9]	**4.6** ± 4.5	[−0.8, 11.5]	0.006
PZ $D_{98\%}$	**42.5** ± 1.0 (Gy)	[39.8, 43.3]	**−12.4** ± 2.8	[−16.4, −5.4]	0.002
Rectum					
D_{Mean}	**10.2** ± 2.9 (Gy)	[5.5, 13.7]	**−39.2** ± 9.0	[−48.0, −18.6]	0.002
V_{40Gy}	**15.2** ± 4.9 (%)	[7.8, 22.2]	**−57.0** ± 9.2	[−63.3, −34.3]	0.002
V_{60Gy}	**6.5** ± 2.4 (%)	[3.2, 10.9]	**−63.7** ± 9.3	[−78.1, −46.9]	0.002
$D_{2\%}$	**33.7** ± 1.5 (Gy)	[31.3, 35.4]	**−12.6** ± 4.2	[−19.0, −7.4]	0.002
Urethra					
D_{Mean}	**33.1** ± 3.3 (Gy)	[27.5, 36.9]	**−2.6** ± 1.2	[−4.7, −0.9]	0.002
$D_{2\%}$	**40.0** ± 0.2 (Gy)	[39.7, 40.5]	**−0.2** ± 0.5	[−1.2, 0.7]	NS
Bladder					
D_{Mean}	**10.2** ± 2.3 (Gy)	[5.1, 13.7]	**−14.4** ± 9.1	[−28.1, −2.5]	0.002
$D_{2\%}$	**36.3** ± 3.0 (Gy)	[27.9, 37.9]	**−5.3** ± 3.7	[−9.8, 0.6]	0.004
Femural heads					
R D_{Mean}	**7.8** ± 2.5 (Gy)	[4.7, 12.3]	**19.9** ± 30.1	[−14.0, 92.1]	NS
R $D_{2\%}$	**15.3** ± 2.0 (Gy)	[12.9, 18.4]	**3.5** ± 13.0	[−11.0, 27.4]	NS
L D_{Mean}	**8.0** ± 1.7 (Gy)	[6.0, 10.8]	**12.7** ± 17.3	[−19.5, 44.5]	0.03
L $D_{2\%}$	**15.2** ± 1.3 (Gy)	[13.8, 17.3]	**2.0** ± 8.7	[−12.2, 12.5]	NS
Other					
V_{10Gy}*	**2274** ± 382 (cc)	[1824, 3163]	**−11.1** ± 2.6	[−15.2, −6.9]	0.002
V_{20Gy}*	**365** ± 67 (cc)	[295, 520]	**−3.4** ± 2.7	[−7.4, 2.2]	0.006
V_{30Gy}*	**178** ± 33 (cc)	[143, 257]	**−4.8** ± 3.0	[−9.4, 0.2]	0.004
CI	**1.2** ± 0.1	[1.1, 1.3]	**−2.5** ± 4.5	[−10.0, 3.1]	NS
MU	**24791** ± 1302	[22624, 26844]	**75.7** ± 9.2	[56.8, 91.7]	0.002

4. Discussion

Recently, we have presented iCycle, our in-house developed algorithm for integrated, multi-criterial optimization of beam angles and profiles (Breedveld *et al* 2012). For plan generation, iCycle uses *a priori* defined plan criteria (wish-list, section 2.4 and table 1) and a beam direction search space. The wish-list is used to fully automatically generate high-quality plans without interactive tweaking of parameters such as weighting factors in the cost function. For a plan with *N* selected orientations, the solution is Pareto optimal regarding the generated beam profiles (Breedveld *et al* 2012, 2009). To ensure generation of clinically acceptable plans with favorable balances in the outcomes for the various plan objectives, wish-lists are developed in close collaboration with treating clinicians. This study is based on 1500 treatment plans generated with iCycle (10 patients, 5 beam sets, 30 beams). Due to the automation, the plan generation workload was minimal and plan quality was independent of the experience and skills of human planners. To our knowledge, this is the first paper investigating in detail the impact of the extent of the beam angle search space on computer optimization of IMRT dose distributions.

For each individual patient, PTV doses in the iCycle generated plans for the five investigated search spaces were highly similar (figures 3–5 and table 2), and tuned to be in close agreement with the clinically delivered dose. This allowed focusing plan comparisons on OARs, and specifically on the highest priority OAR, the rectum. Rectum doses for all four NCP beam direction search spaces were clearly superior when compared to doses obtained with the CP search space (figures 3–6 and table 2). Also for the femoral heads, V_{10Gy} and V_{30Gy}, NCP plans performed better (table 2). CP plans had (slightly) improved V_{30Gy}, CI and MU.

The CK^{+} and CK^{++} search spaces were used to study dosimetrical consequences of limitations in the extent of the CK space (figure 1, sections 2.3, 3.4 and 3.5). The data presented in section 3.4 do clearly demonstrate that extension of the CK space to include beams with larger direction components along the superior–inferior axis could substantially enhance plan quality ($CK^{+} \rightarrow CK^{++}$). On the other hand, further addition of beams with larger posterior components did not improve plans ($CK^{++} \rightarrow$ F-NCP). Comparison of the right panels in figures 7 and 8 shows that also in the case of availability of the posterior beams (F-NCP), most selected high-weight beams are within the borders of the CK^{++} space that lacks posterior beams. As plan quality for F-NCP and CK^{++} is highly similar, it may be concluded that omission of posterior beams does not limit the quality of generated plans.

As demonstrated in figures 4 and 5, for all search spaces, plan quality continued to improve with increasing numbers of involved beams, with some leveling off for >20 beams. Table 3 details the very significant improvements that can be obtained with 25 CP beam configurations compared to 11 CP beams. This observation might seem in striking contrast with the broadly applied $\leqslant 9$ beams for prostate in clinical practices. However, it has to be considered here that HDR like dose distributions were investigated in this paper, aiming at highly inhomogeneous PTV doses with some sparing of the urethra and enhanced dose delivery in the PZ. In an on-going study, we are investigating the use of large numbers of beams for more regular prostate IMRT dose distributions.

Also for very large beam numbers, NCP configurations clearly performed better than CP set-ups (figures 5 and 6, table 2). On conventional treatment units with L-shaped gantries, delivery of NCP plans with many beams would result in impractically long treatment times and a high workload because of the involved couch rotations. The latter would also limit treatment accuracy. The performed treatment time calculations for a robotic CK equipped with an MLC (sections 2.6 and 3.6) demonstrated that treatment times of around 18 min could be obtained with such a system, including intra-fraction imaging and position correction prior to delivery of each of the 25 beams.

As mentioned in section 2.4, for each patient, PTV doses in iCycle plans were highly similar to the dose in the plan generated with the clinical treatment planning system for actual treatment with the CK. On the other hand, it was observed that rectum doses in iCycle plans were highly superior to corresponding doses in the clinical plans (not described in detail in this paper). This may seem unexpected for the CK search space that contains the feasible beam directions of the CK treatment unit. A possible explanation may be that clinical plans were generated with three circular cones per patient, while for the iCycle simulations, it was assumed that beam collimation was performed with an MLC. These observations are now being investigated in great detail, to be reported in a separate paper.

In this study, minimization of the mean rectum dose was used as the highest priority objective, aiming at rectum sparing (table 1). Many studies have been performed to establish plan parameters that correlate most with rectum toxicity, see Michalski *et al* (2010) for an overview. The QUANTEC group suggests V_{60}, but using this objective directly in the optimization leads to less desirable results because of the focus on a single dose-point. Instead,

we used rectum D_{Mean} as an objective in the optimizations, while V_{60} was included in plan evaluations.

In iCycle, the wish-list is used to generate plans with favorable balances between the various treatment goals. In our investigations, we imposed a very strong drive for minimization of the mean rectum dose (table 1: priority 3, goal: 0 Gy). Such a focus on rectum dose minimization has a danger that slightly higher rectum doses could potentially result in (unobserved) much improved doses to other OAR. In the trial plan generations for creating the applied wish-list (section 2.4), no evidence was found that this would actually occur. In the near future, we will however study the value of navigation tools (Monz *et al* 2008, Craft and Bortfeld 2008, Teichert *et al* 2011) for exploring the solution space around iCycle generated plans. Anyway, as in this study the same wish-list was used for all search spaces, numbers of involved beams and patients, it is believed that the impact of not performing navigation on main conclusions of the work will be minimal.

In this paper, we compared plan quality of treatments with up to 30 optimized CP beam directions with optimized NCP techniques. There is no existing machine that can deliver treatments for all investigated beam search spaces. The CK search space does not include 72 equi-angular CP beams, neither does it contain all directions defined for CK^{+} and CK^{++}. The fully non-coplanar (F-NCP) space cannot be realized with any of the commercially available systems, e.g. because of linac-bunker floor collisions, gantry-couch collisions or beams going through heavy couch elements. However, the F-NCP dose distributions give an upper limit of what could theoretically be obtained with optimized NCP set-ups. To make conclusions on the impact of the beam search space on plan quality independent of the applied optimizer, the type of beam shaping, and the beam characteristics, all optimizations were performed with the iCycle optimizer, using the same dose calculation engine for the same MLC (section 2.4).

Optimization results may depend on dose calculation accuracy (Jeraj *et al* 2002). It is well known that dose calculations using pencil beams and equivalent path length correction have limited accuracy, especially in low-density tissues. In this study on prostate cancer, these tissues were largely absent in the treatment fields. Moreover, the same dose calculation algorithm was used for all beam direction search spaces. Therefore, we believe that limitations in the applied dose calculation engine do not jeopardize our main conclusions on ranking of the beam search spaces.

As described in section 3.8, optimization times were long, especially for the largest NCP search spaces. There are many possibilities for substantial reductions and this is an area of active research in our group. On the other hand, based on an *a priori* defined, fixed wish-list per patient group, iCycle optimized plans are generally of very high quality, and do not require further iterations with new iCycle runs (Breedveld *et al* 2012) (as explained in section 2.4, in this study, PTV constraints and objectives were tuned per patient to reproduce different clinical PTV dose distributions). In a recent prospective clinical study for evaluation of iCycle in head and neck IMRT, for each patient the treating physician was presented with a plan based on iCycle and a plan made by dosimetrists with the clinical treatment planning system. In 32 out of 33 plan selections, the treating physician selected the iCycle-based plan. Also objectively, the latter plans were clearly of higher quality (Voet *et al* 2012b). This study focused on generation of prostate SBRT plans that mimicked HDR brachytherapy dose distributions. Conclusions on the importance of NCP beams, on the favorable use of large numbers of beams (>20) and on the limited importance of posterior beams may not be valid in other circumstances. Recently, we demonstrated for a group of head and neck cancer patients that inclusion of NCP beams in the search space did only marginally improve IMRT plans (Voet *et al* 2012a). Studies for other treatment sites are on-going.

5. Conclusion

For prostate SBRT, IMRT plans generated with all four investigated non-coplanar search spaces had clearly improved organ at risk (OAR) sparing compared to the coplanar (CP) search space, especially for the rectum which was the most important OAR in this study. OAR sparing was best with the fully non-coplanar (F-NCP) search space, with improvements in rectum D_{Mean}, $V_{40\text{Gy}}$, $V_{60\text{Gy}}$ and $D_{2\%}$ compared to CP of 25%, 35%, 37% and 8%, respectively. Reduced rectum sparing with the CK search space compared to F-NCP could be largely compensated by extending the CK space with beams with relatively large direction components along the superior–inferior axis (CK^{++}). Further addition of posterior beams to define the F-NCP search space did not result in plans with clinically relevant further reductions in OAR sparing. Plans with 25 beams clearly performed better than plans with only 11 beams. For CP set-ups, an increase in involved number of beams from 11 to 25 resulted in reductions in rectum D_{Mean}, $V_{40\text{Gy}}$, $V_{60\text{Gy}}$ and $D_{2\%}$ of 39%, 57%, 64% and 13%, respectively.

References

Alber M and Reemtsen R 2007 Intensity modulated radiotherapy treatment planning by use of a barrier-penalty multiplier method *Optim. Methods Softw.* **22** 391–411

Aleman D M, Romeijn H E and Dempsey J F 2009 A response surface approach to beam orientation optimization in intensity modulated radiation therapy treatment planning *INFORMS J. Comput.* **21** 62–76

Aluwini S, van Rooij P, Hoogeman M, Bangma C, Kirkels W J, Incrocci L and Kolkman-Deurloo I K 2010 CyberKnife stereotactic radiotherapy as monotherapy for low- to intermediate-stage prostate cancer: early experience, feasibility and tolerance *J. Endourol.* **24** 865–9

Arcangeli G, Fowler J, Gomellini S, Arcangeli S, Saracino B, Petrongari M, Benassi M and Strigari L 2011 Acute and late toxicity in a randomized trial of conventional versus hypofractionated three-dimensional conformal radiotherapy for prostate cancer *Int. J. Radiat. Oncol. Biol. Phys.* **79** 1013–21

Blomgren H, Lax I, Naslund I and Svanstrom R 1995 Stereotactic high dose fraction radiation therapy of extracranial tumours using an accelerator *Acta Oncol.* **34** 861–70

Breedveld S, Storchi P R M, Keijzer M, Heemink A W and Heijmen B J M 2007 A novel approach to multi-criteria inverse planning for IMRT *Phys. Med. Biol.* **52** 6339–53

Breedveld S, Storchi P and Heijmen B 2009 The equivalence of multi-criteria methods for radiotherapy plan optimization *Phys. Med. Biol.* **54** 7199–209

Breedveld S, Storchi P, Voet P and Heijmen B 2012 iCycle: integrated, multicriterial beam angle, and profile optimization for generation of coplanar and noncoplanar IMRT plans *Med. Phys.* **39** 951–63

Brenner D and Hall E 1999 Fractionation and protraction for radiotherapy of prostate carcinoma *Int. J. Radiat. Oncol. Biol. Phys.* **43** 1095–101

Craft D and Bortfeld T 2008 How many plans are needed in an IMRT multi-objective plan database? *Phys. Med. Biol.* **53** 2785–96

de Pooter J A, Méndez Romero A, Wunderink W, Storchi P R M and Heijmen B J M 2008 Automated non-coplanar beam direction optimization improves IMRT in SBRT of liver metastasis *Radiother. Oncol.* **88** 376–81

Demanes D, Rodriguez R, Schour L, Brandt D and Altieri G 2005 High-dose-rate intensity-modulated brachytherapy with external beam radiotherapy for prostate cancer: California endocurietherapy's 10-year results *Int. J. Radiat. Oncol. Biol. Phys.* **61** 1306–16

Fowler J, Chappell R and Ritter M 2001 Is alpha/beta for prostate tumors really low? *Int. J. Radiat. Oncol. Biol. Phys.* **50** 1021–31

Freeman D and King C 2011 Stereotactic body radiotherapy for low-risk prostate cancer: five-year outcomes *Radiation Oncology* **6** 3

Freeman D E, Friedland J L and Masterson-McGary M E 2010 Stereotactic radiosurgery for low-intermediate risk prostate cancer: an emerging treatment approach *Am. J. Clin. Oncol.* **33** 208

Fuller D, Mardirossian G, Wong D and McKellar H 2010 Prospective evaluation of CyberKnife stereotactic body radiotherapy for low- and intermediate-risk prostate cancer: emulating HDR brachytherapy dose distribution *Int. J. Radiat. Oncol. Biol. Phys.* **78** 5358–9

Fuller D B, Naitoh J, Lee C, Hardy S and Jin H 2008 Virtual HDR Cyberknife treatment for localized prostatic carcinoma: dosimetry comparison with HDR brachytherapy and preliminary clinical observations *Int. J. Radiat. Oncol. Biol. Phys* **70** 1588–97

Grills I, Martinez A, Hollander M, Huang R, Goldman K, Chen P and Gustafson G 2004 High dose rate brachytherapy as prostate cancer monotherapy reduces toxicity compared to low dose rate palladium seeds *J. Urol.* **171** 1098–104

ICRU 2010 Prescribing, Recording, and Reporting Photon-Beam Intensity-Modulated Radiation Therapy (IMRT) *ICRU Report 83* vol 10 (Oxford: Oxford University Press)

Jabbari S *et al* 2012 Stereotactic body radiotherapy as monotherapy or post-external beam radiotherapy boost for prostate cancer: technique, early toxicity, and PSA response *Int. J. Radiat. Oncol. Biol. Phys.* **82** 228–34

Jeraj R, Keall P J and Siebers J V 2002 The effect of dose calculation accuracy on inverse treatment planning *Phys. Med. Biol.* **47** 391–407

Katz A and Santoro M 2009 CyberKnife radiosurgery for early carcinoma of the prostate: a three year experience *Int. J. Radiat. Oncol. Biol. Phys.* **75** S312–3

Kilby W, Dooley J R, Kuduvalli G, Sayeh S, Maurer J and R C 2010 The CyberKnife robotic radiosurgery system in 2010 *Technol. Cancer Res. Treat.* **9** 433–52

King C, Lehmann J, Adler J and Hai J 2003 CyberKnife radiotherapy for localized prostate cancer: rationale and technical feasibility *Technol. Cancer Res. Treat.* **2** 25–30

King C and Fowler J 2001 A simple analytic derivation suggests that prostate cancer alpha/beta ratio is low *Int. J. Radiat. Oncol. Biol. Phys.* **51** 213–4

King C, Brooks J, Gill H and Presti J 2011 Long-term outcomes from a prospective trial of stereotactic body radiotherapy for low-risk prostate cancer *Int. J. Radiat. Oncol. Biol. Phys.* **82** 877–82

Michalski J, Gay H, Jackson A, Tucker S and Deasy J 2010 Radiation dose-volume effects in radiation-induced rectal injury *Int. J. Radiat. Oncol. Biol. Phys.* **76** S123–9

Miralbell R, Roberts S, Zubizarreta E and Hendry J 2012 Dose-fractionation sensitivity of prostate cancer deduced from radiotherapy outcomes of 5969 patients in seven international institutional datasets: $\alpha/\beta = 1.4$ (0.9–2.2) Gy *Int. J. Radiat. Oncol. Biol. Phys.* **82** e17–24

Monz M, Küfer K H, Bortfeld T R and Thieke C 2008 Pareto navigation—algorithmic foundation of interactive multi-criteria IMRT planning *Phys. Med. Biol.* **53** 985–98

Norkus D, Miller A, Kurtinaitis J, Haverkamp U, Popov S, Prott F and Valuckas K 2009 A randomized trial comparing hypofractionated and conventionally fractionated three-dimensional external-beam radiotherapy for localized prostate adenocarcinoma: a report on acute toxicity *Strahlenther. Onkol.* **185** 715–21

Pollack A *et al* 2006 Dosimetry and preliminary acute toxicity in the first 100 men treated for prostate cancer on a randomized hypofractionation dose escalation trial *Int. J. Radiat. Oncol. Biol. Phys.* **64** 518–26

Pugachev A and Xing L 2001 Computer-assisted selection of coplanar beam orientations in intensity-modulated radiation therapy *Phys. Med. Biol.* **46** 2467–76

Storchi P and Woudstra E 1996 Calculation of the absorbed dose distribution due to irregularly shaped photon beams using pencil beam kernels derived from basic beam data *Phys. Med. Biol.* **41** 637–56

Teichert K, Süss P, Serna J I, Monz M, Küfer K H and Thieke C 2011 Comparative analysis of Pareto surfaces in multi-criteria IMRT planning *Phys. Med. Biol.* **56** 3669–84

Townsend N, Huth B, Ding W, Garber B, Mooreville M, Arrigo S, Lamond J and Brady L 2011 Acute toxicity after CyberKnife-delivered hypofractionated radiotherapy for treatment of prostate cancer *Am. J. Clin. Oncol.* **34** 6–10

van de Water S, Hoogeman M S, Breedveld S and Heijmen B J M 2011 Shortening treatment time in robotic radiosurgery using a novel node reduction technique *Med. Phys.* **38** 1397–405

van Santvoort J P C and Heijmen B J M 1996 Dynamic multileaf collimation without 'tongue-and-groove' underdosage effects *Phys. Med. Biol.* **41** 2091–105

Voet P, Breedveld S, Dirkx M, Levendag P and Heijmen B 2012a Integrated multi-criterial optimization of beam angles and intensity profiles for coplanar and non-coplanar head and neck IMRT and implications for VMAT *Med. Phys.* **39** 4858

Voet P, Dirkx M, Breedveld S, Fransen D, Levendag P and Heijmen B 2012b Towards fully automated multi criterial plan generation: a prospective clinical study *Int. J. Radiat. Oncol. Biol. Phys.* (at press) doi: 10.1016/j.ijrobp.2012.04.015

Woudstra E and Storchi P R M 2000 Constrained treatment planning using sequential beam selection *Phys. Med. Biol.* **45** 2133–49

Yeoh E, Botten R, Butters J, Di Matteo A, Holloway R and Fowler J 2011 Hypofractionated versus conventionally fractionated radiotherapy for prostate carcinoma: final results of phase III randomized trial *Int. J. Radiat. Oncol. Biol. Phys.* **81** 1271–8